Electronic Supplementary Information for

A MnOx-nucleic acid nanoprobe with enzyme-free cascade signal amplification for ultrasensitive intracellular microRNA imaging

Jiayao Xu‡, Yuxin Qin‡, Qiuyi Liang, Xiaohong Zhong, Li Hou, Yong Huang*, Shulin Zhao and Hong Liang**

School of Chemistry and Pharmaceutical Sciences, State Key Laboratory for the Chemistry and Molecular Engineering of Medicinal Resources, Guangxi Normal University, Guilin 541004, P. R. China.

E-mail: houli@gxnu.edu.cn; huangyong_2009@163.com; hliang@gxnu.edu.cn

Fax: +86-773-5832294; Tel: +86-773-5856104

Experimental section

Chemicals and reagents

Potassium permanganate ($KMnO_4$) was a homemade analytical pure reagent. Polyallylamine hydrochloride (PAH) and Dimethyl sulfoxide (DMSO) were purchased from Sigma-Aldrich (St. Louis, MO, USA). 100×penicillin-streptomycin mixture, tetramethylazolium salt (MTT) and trypsin were purchased from Solarbio Technology Co., Ltd. (Beijing, China); PBS buffer and DMEM culture medium were purchased from Thermo Fisher Scientific Technology Co., Ltd. (USA). DAPI was purchased from Biyuntian Biotechnology Co., Ltd. (Shanghai, China). Fetal bovine serum (FBS) was purchased from ExCell Biotechnology Co., Ltd. (China). Glutathione (GSH) was purchased from Sigma-Aldrich (St. Louis, MO, USA). Ammonium persulfate, acrylamide, coagulant tetramethylenediamine (TEMED), electrophoresis buffer solution, standard DNA were purchased from Aladdin Reagent Co., Ltd. (Shanghai, China). SybrGreen PCR Master Mix was purchased from ABI (USA). AMV First Strand cDNA Synthesis Kit was purchased from BBI (Toronto, Canada). The solution of oligonucleotide was 1×TE buffer. Tris-HCl buffer was used as diluent and detection solution. The nucleic acid chain was synthesized by Sangon Biotech (Shanghai, China) and purified by High Performance Liquid Chromatography (HPLC). The biological ultrapure water (18.2 MΩ·cm) was purified by the Milli-Q water purification system (Milli-Q, Millipore, USA). The DNA sequences were shown in Table S1.

Table S1. Oligonucleotide sequence (5'→3')

Oligonucleotides	Sequences
miRNA-21（T）	UAG CUU AUC AGA CUG AUG UUGA
H1	CAT AAG ACT TCT TCA ACA-Cy5-TCA GTC TGA TAA GCT ACA CAA CTA GCT TAT CAG AC TGA-BHQ2-TAT TGA
H2	CAT AAG ACT TCT TCA GTC TGA TAA GCT AGT TGT GGA CTG ATG TTG ACA CAA CTA GCT ATT GA
H3	CAT AAG ACT TCT GCT AGT TGT GTC AAC ATC AGT CTA GCT TAT CAG ACT GAT GTT GAT ATT GA
H4	CTG CTC AGC GAT CCT TCT-Cy5-TAT TGA AAG TTA TTA ATC AAT-BHQ2-AAG AAG TCT TAT GAA GGC ACC CAT GTA GTC AA
H4-1	CTG CTC AGC GAT CCT TCT-Cy3-TAT TGA AAG TTA TTA ATC AAT-BHQ2-AAG AAG TCT TAT GAA GGC ACC CAT GTA GTC AA
H5	CTG CTC AGC GAT CCT TTT AAT AAC TTT CAA TAA GCA TAA GAC TTC TTA TTG AAA GGC ACC CAT GTA GTC AA
S	TAG CTT ATC AGA CTG ATG TTG ACT TrAG GAG CAG TTA GGC TAT TCG GCA CAA GTG G
S-1	TAG CTT ATC AGA CTG ATG TTG ACT TrAG GAG CAG TTA GGC TAT TCG GCA CAA GTG G-FAM
L	CCA CTT GTG CCG AAT AGC CTA AAA GAT AAA GCT A
L-1	DABCYL-CCA CTT GTG CCG AAT AGC CTA AAA GAT AAA GCT A
miRNA-219	UGAUUGUCCAAACGCAAUUCU
miRNA-141	UAACACUGUCUGGUAAAGAUGG
miRNA-223	UGUCAGUUUGUCAAAUACCCC
Forward primer for miRNA-21	GCGCTAGCTTATCAGACTGA
Reverse primer for miRNA-21	GTGCAGGGTCCGAGGT

Apparatus

H1650-W high-speed micro centrifuge (Hunan Xiangyi centrifuge instrument Co., Ltd.); DF-101S heat-collecting constant temperature heating magnetic mixer (Gongyi Yuhuayi Co., Ltd.); DHG electrothermal constant temperature blast drying oven (Shanghai Jinhong Experimental equipment Co., Ltd.); carbon dioxide incubator (Hamamatsu, Japan); FA604A electronic balance (Shanghai Jingtian Electronic instrument Co., Ltd.). SZCL-2A Digital display Intelligent temperature controlled Magnetic heating Mixer (Gongyi Yuhua instrument Co., Ltd.); XW-80A Vortex Oscillation Mixer (instrument Factory of Shanghai Medical University); Talos200S Field Emission Transmission Electron microscope (Thermo Fisher Scientific Company; USA); Cary60 Ultraviolet Spectrophotometer (Agilent Technologies Inc Company, USA); KQ5200B Ultrasonic Cleaner (Kunshan Ultrasonic instrument Co., Ltd.); BD FACSAriall flow Cytometer (BD Company, USA). LSM710 laser confocal microscope-living cell workstation (Zeiss company, Germany); LS-55 fluorescence spectrophotometer (Perkin-Elmer company, USA); Laser particle size analyzer (Shanghai Sibaiji instrument system Co., Ltd.); El×800 enzyme labeling instrument (Bio Tekinstruments company, USA); DYY-8C electrophoresis instrument (Beijing Liuyi instrument Factory); Omega16ic gel imaging analysis system; CFX96TM Real-Time System (Bio-Rad，USA). The biological cell samples that we used for our experiment were obtained from the National Collection of Authenticated Cell Cultures (Shanghai, China). All experiments were performed in compliance with the relevant laws and institutional guidelines, and the institutional committee has approved the experiments.

Preparation of MnOx nanoparticles

MnOx nanozyme was prepared according to methods reported in literature.[1] PAH (0.0179 g) was dissolved in 10 mL of deionized water and stirred at room temperature for 10 min. Then KMnO4 (0.0075 g) was added in the above solution and stirred at room temperature for 10 min until the color of the solution changes from purple to brown. The above resulting solution was transferred to a thermostat water bath at 75 ℃ and continued the reaction for 0.5 h. The prepared MnOx nanozyme was washed and centrifuged with anhydrous ethanol for six times (8000 rpm, 10 min), and finally dispersed in water. The resulting MnOx nanozyme (1 $mg \cdot mL^{-1}$) was placed in an ultrasonic instrument for 6 h, and stored at room temperature.

Preparation of MnOx nanoprobe

The MnOx nano-probe was prepared by the physical adsorption between MnOx nanoparticles and DNA chain phosphate skeleton. Firstly, the prepared MnOx nanoparticles (80 μL, 1 $mg \cdot mL^{-1}$), H1 hairpin (100 μL, 20 $\mu mol \cdot L^{-1}$), H2 hairpin (100 μL, 20 $\mu mol \cdot L^{-1}$), H3 hairpin (100 μL, 20 $\mu mol \cdot L^{-1}$), H4 hairpin (100 μL, 20 $\mu mol \cdot L^{-1}$), H5 hairpin (100 μL, 20 $\mu mol \cdot L^{-1}$) and H6 substrate hairpin (100 μL, 20 $\mu mol \cdot L^{-1}$, formed by the combination of single-stranded S and single-stranded L) were added to 320 μL of Tris-HCl buffer (10 $mmol \cdot L^{-1}$ Tris-HCl, 20 $mmol \cdot L^{-1}$ NaCl, 20 $mmol \cdot L^{-1}$ $MgCl_2$, pH 7.4) and incubated at 37 ℃ for 1 h. The MnOx-CHA-HCR-DNAzyme nanoprobe can be obtained. The MnOx-H1 nanoprobe (the absence of H2, H3, H4, H5 and H6), MnOx-CHA nanoprobe (the absence of H4, H5 and H6), The MnOx-CHA-HCR nanoprobe (the absence of H2, H3, H4 and H5) is also obtained by using the

similar method mentioned above, respectively.

Study on the release of Mn^{2+} under different GSH concentrations

The MnOx nanoparticles (80 μL, 1 mg·mL^{-1}) were added to a glutathione (GSH) solution (100 μL, 40 mmol L^{-1}) for complete dissolution, and they were used as control group. Then, different concentrations of GSH (0, 0.4, 0.8, 1.2, 1.6, 2.0 mmol·L^{-1}) was added into 80 μL of MnOx nanoparticles (1 mg·mL^{-1}), respectively. All the above samples were diluted to 1 mL with PBS buffer (pH 5.5) and incubated for 6 h. All samples were centrifuged at 8000 rpm for 10 min. The supernatant was prepared and diluted 2500 times with ultra-pure water. Finally, all diluted samples were used for ICP-MS determination.

Fluorescence detection of miRNA-21 in vitro

The sample preparation process was as follows: (1) sample a (CHA sensing system): H1 (10 μL, 2 μ mol·L^{-1}), H2 (10 μL, 2 μmol·L^{-1}) and H3 (10 μL, 2 μmol·L^{-1}) were added to the 160 μL of Tris-HCl （5 mmol·L^{-1} Mn^{2+}） buffer solution. (2) sample b (CHA-HCR sensing system): H1 (10 μL, 2 μmol·L^{-1}), H2 (10 μL, 2 μmol·L^{-1}), H3 (10 μL, 2 μmol·L^{-1}), H4 (10 μL, 2 μmol·L^{-1}) and H5 (10 μL, 2 μmol·L^{-1}) were added to the 140 μL of Tris-HCl （5 mmol·L^{-1} Mn^{2+}） buffer solution. (3) sample c (CHA-HCR-DNAzyme sensing system): H1 (10 μL, 2 μmol·L^{-1}), H2 (10 μL, 2 μmol·L^{-1}), H3 (10 μL, 2 μmol·L^{-1}), H4 (10 μL, 2 μmol·L^{-1}), H5 (10 μL, 2 μmol·L^{-1}) and H6 substrate hairpin (10 μL, 2 μmol·L^{-1}) were added to 130 μL of Tris-HCl （5 mmol·L^{-1} Mn^{2+}） buffer solution.

10 μL of different concentrations of miRNA-21 was added to sample a, sample b and

sample c, respectively. Subsequently, all the samples were incubated in a thermostat water bath at 37 ℃ for 2.5 h. The fluorescence of Cy5 was detected by fluorescence spectrophotometer. The detection conditions of the above samples were as follows: excitation wavelength at 633 nm, emission wavelength at 660 nm, slit width at 10 nm.

The percentage (A) of fluorescence signal increase from different sensing systems was calculated as follows:

$$A=[(I-I_0)/I_0]\times 100\%.$$

I was the fluorescence intensity of the sensing system after introduction of the target miRNA-21. I_0 was fluorescence intensity of the sensing system in the absence of the target miRNA-21.

Fluorescence detection of miRNA-21 in cell lysates

H1 (10 μL, 2 μmol·L^{-1}), H2 (10 μL, 2 μmol·L^{-1}), H3 (10 μL, 2 μmol·L^{-1}), H4 (10 μL, 2 μmol·L^{-1}), H5 (10 μL, 2 μmol·L^{-1}) and H6 substrate hairpin (10 μL, 2 μmol·L^{-1}) were added to 130 μL of Tris-HCl （5 mM Mn^{2+}） buffer solution. 10 μL of different concentrations of T24 cell lysate was added to sample.

H1 (10 μL, 2 μmol·L^{-1}), H2 (10 μL, 2 μmol·L^{-1}), H3 (10 μL, 2 μmol·L^{-1}), H4 (10 μL, 2 μmol·L^{-1}), H5 (10 μL, 2 μmol·L^{-1}) and H6 substrate hairpin (10 μL, 2 μmol·L^{-1}) were added to 130 μL of Tris-HCl （5 mM Mn^{2+}） buffer solution. 10 μL of different cell lines (T24, MCF-7, HeLa, HCV-29, MCF-10A and 3T3) of cell lysate was added to sample, respectively.

Subsequently, all the samples were incubated in a thermostat water bath at 37 ℃

for 2.5 h. The fluorescence of Cy5 was detected by fluorescence spectrophotometer. The detection conditions of the above samples were as follows: excitation wavelength at 633 nm, emission wavelength at 660 nm, slit width at 10 nm.

Fluorescence detection of DNAzyme activation in vitro

The sample preparation process was as follows: (1) sample a: H1 (10 μL, 2 μmol·L^{-1}), H2 (10 μL, 2 μmol·L^{-1}), H3 (10 μL, 2 μmol·L^{-1}), H4 (10 μL, 2 μmol·L^{-1}), H5 (10 μL, 2 μmol·L^{-1}) and H6-1 (S-1, L-1) substrate hairpin (10 μL, 2 μmol·L^{-1}) were added to 140 μL of Tris-HCl buffer solution; (2) sample b: H1 (10 μL, 2 μmol·L^{-1}), H2 (10 μL, 2 μmol·L^{-1}), H3 (10 μL, 2 μmol·L^{-1}), H4 (10 μL, 2 μmol·L^{-1}), H5 (10 μL, 2 μmol·L^{-1}) and H6-1 (S-1, L-1) substrate hairpin (10 μL, 2 μmol·L^{-1}) were added to 140 μL of Tris-HCl buffer solution (5 mmol·L^{-1} Mn^{2+}); (3) sample c: H1 (10 μL, 2 μmol·L^{-1}), H2 (10 μL, 2 μmol·L^{-1}), H3 (10 μL, 2 μmol·L^{-1}), H4 (10 μL, 2 μmol·L^{-1}), H5 (10 μL, 2 μmol·L^{-1}), H6-1 (S-1, L-1) substrate hairpin (10 μL, 2 μmol·L^{-1}) and miRNA-21 (10 μL, 0.2 μmol·L^{-1}) were added to 130 μL of Tris-HCl buffer solution; (4) sample c: H1 (10 μL, 2 μmol·L^{-1}), H2 (10 μL, 2 μmol·L^{-1}), H3 (10 μL, 2 μmol·L^{-1}), H4 (10 μL, 2 μmol·L^{-1}), H5 (10 μL, 2 μmol·L^{-1}), H6-1 (S-1, L-1) substrate hairpin (10 μL, 2 μmol·L^{-1}) and miRNA-21 (10 μL, 0.2 μmol·L^{-1}) were added to 130 μL of Tris-HCl buffer solution (5 mmol $L^{-1}$$Mn^{2+}$).

Polyacrylamide gel electrophoresis analysis

Polyacrylamide gel electrophoresis was used to verify the reaction feasibility of the

CHA-HCR-DNAzyme sensing system. Samples for gel electrophoresis assays were prepared as follows: (1) H1 (2.0 μM), H2 (2.0 μM) and H3 (2.0 μM) were used as samples one, two and three respectively; (2) the mixture of H1 (2.0 μM) and H2 (2.0 μM) was incubated for 150 min at 37 ℃, the resulting mixture was used as sample four; (3) the mixture of H1 (2.0 μM), H2 (2.0 μM) and H3 (2.0 μM) was incubated for 150 min at 37 ℃, the resulting mixture was used as sample; (4) the mixture of H1 (2.0 μM) and miRNA-21 (1.0 μM) was incubated for 150 min at 37 ℃, and the resulting mixture was used as sample six; (5) the mixture of H1 (2.0 μM), H2 (2.0 μM) and miRNA-21 (1.0 μM) was incubated for 150 min at 37 ℃, the resulting mixture was used as sample senven; (6) the mixture of H1 (2.0 μM), H2 (2.0 μM) , H3 (2.0 μM) and miRNA-21 (1.0 μM) the resulting mixture was used as sample eight; (7) miRNA-21 (1.0 μM), H4 (2.0 μM) and H2 (2.0 μM) were used as samples nine, ten and eleven respectively; (8) the mixture of H4 (2.0 μM) and H5 (2.0 μM) was incubated for 150 min at 37 ℃, the resulting mixture was used as sample twelve; (9) the mixture of H1 (2.0 μM), H2 (2.0 μM) , H3 (2.0 μM), H4 (2.0 μM) and H5 (2.0 μM) the resulting mixture was used as sample thirteen; (10) the mixture of H1 (2.0 μM), H2 (2.0 μM) , H3 (2.0 μM), H4 (2.0 μM) and miRNA-21 (1.0 μM) the resulting mixture was used as sample fourteen; (10) the mixture of H1 (2.0 μM), H2 (2.0 μM) , H3 (2.0 μM), H4 (2.0 μM), H5 (2.0 μM) and miRNA-21 (1.0 μM) the resulting mixture was used as sample fifteen; (11) the mixture of H1 (2.0 μM), H2 (2.0 μM) , H3 (2.0 μM), H4 (2.0 μM), H5 (2.0 μM), H6 (2.0 μM) and miRNA-21 (1.0 μM) the resulting mixture was used as sample sixteen; (12) L (1.0 μM) was used as sample seventeen; (13) H6 (2.0 μM) were used as samples eighteen.;

(14) the mixture of H1 (2.0 μM), H2 (2.0 μM) , H3 (2.0 μM), H4 (2.0 μM), H5 (2.0 μM) and H6 (2.0 μM) the resulting mixture was used as sample sixteen; (15) L (1.0 μM) was used as sample seventeen. All samples contained 5 mmol L^{-1} Mn^{2+}. For PAGE analysis, 8 μL each prepared samples was put on a 15% Polyacrylamide gel, and electrophoresis was performed in 1×TBE buffer (pH 7.9) at 80 V constant voltage for 90 min. After that, the gel was stained by ethidium bromide and scanned by the digital camera.

Confocal fluorescence imaging of cells

Cell imaging experiment at different incubation time: 2 mL of digested T24 tumor cells was planted in a cell petri dish. When the cell density reached 70%, 100 μL of MnOx nanoprobes (the final concentration of MnOx nanoparticles was 80 $\mu g \cdot mL^{-1}$, and the final concentration of each hairpin probe was 100 nmol L^{-1}) and 2 μL, 5 $\mu mol \cdot L^{-1}$ of nuclear staining reagent DAPI were added to the dish. The cell petri dish was incubated in the incubator for different time, taken out, and washed three times with PBS. The culture medium was washed off and the cells were imaged by laser confocal microscope. Among them, the excitation wavelength of DAPI was 405, and the fluorescence signal with emission wavelength of 410~480 nm was collected, and the excitation wavelength of Cy5 was 633 nm, and the acquisition and emission wavelength were 640 nm-740 nm.

Fluorescence imaging of different cell lines treated with different nanoprobes: 2 mL of digested T24 cells, HCV29 cells, HepG-2 cells, HL-7702 cells, HeLa cells and 3T3 cells were seeded in a cell petri dish. When the cell density grew to 70%, 200 μL of

MnOx nanoprobes (the final concentration of MnOx nanoparticles was 80 μg·mL^{-1}, the final concentration of H1, H2, H3, H4, H5, H6 substrate hairpin probes was 100 nmol·L^{-1}) were added into the cell petri dish of different cells, and then 2 μL, 5 μmol·L^{-1} of DAPI staining reagent was added to each cell petri dish. The cell petri dish was incubated in the incubator for 6 h, then washed the petri dish with PBS for three times, washed off culture medium, and then used laser confocal microscope for fluorescence imaging of the cells. The excitation wavelength of DAPI was 405, and the fluorescence signal with emission wavelength of 410~480 nm was collected. The excitation wavelength of Cy5 was 633 nm, and the emission wavelength was 640 nm~740 nm. The fluorescence intensity of different cell lines in different sensing systems was obtained by the laser confocal microscope-living cell workstation.

The experiment of co-incubating normal cells with tumor cells: 2 mL of digested normal cells (HCV-29 cells) were planted in a petri dish. When the cells grew to 40% in the incubator, the culture medium was abandoned, 2 mL of digested T24 cells were added to the petri dish and mixed well. After that, the petri dish was placed in the incubator to continue culture. When the cell density reached 75%, 200 μL of MnOx-CHA-HCR-DNAzyme nanoprobe (the final concentration of MnOx nanoparticles was 80 μg·mL^{-1}, the final concentration of H1, H2, H3, H4, H5, H6 substrate hairpin probe was 100 nmol·L^{-1}) and 2 μL, 5 μmol·L^{-1} of DAPI staining reagent were added to the cell petri dish. The cell petri dish was incubated in the incubator for 6 h, then washed the petri dish with PBS for three times, washed off the culture medium, and then used laser confocal microscope for fluorescence imaging of the cells. The excitation

wavelength of DAPI was 405nm, and the fluorescence signal with emission wavelength of 410 nm~480 nm was collected. The excitation wavelength of Cy5 was 633 nm, and the fluorescence signal with emission wavelength of 640 nm~740 nm was collected.

miRNA-21 down-regulation and up-regulation cell imaging experiment: miRNA-21i and miRNA-21 mimics was transfected into tumor cells by liposome-3000, respectively. And cell imaging experiment was carried out. First, 2 mL of T24 cells were cultured in a petri dish for 6 h. Then liposome-3000 containing miRNA-21i and miRNA-21 mimics was added and incubated in an incubator containing 5% CO_2 at 37 ℃ for 24 h, respectively. After washing with PBS for 3 times, the new medium was replaced, and 200 μL of MnOx-CHA-HCR-DNAzyme nanoprobe (the final concentration of MnOx nanoparticles was 80 $\mu g \cdot mL^{-1}$, the final concentration of H1, H2, H3, H4, H5, H6 substrate hairpin probe was 100 $nmol \cdot L^{-1}$) and 2 μL, 5 $\mu mol \cdot L^{-1}$ of DAPI staining reagent were added into the cell petri dish. The petri dish was incubated in the incubator for 6 h, then the petri dish was washed three times with PBS. The culture medium was washed off, and the cells were imaged by laser confocal microscope. The excitation wavelength of DAPI was 405 nm, and the fluorescence signal with emission wavelength of 410 nm~480 nm was collected. The excitation wavelength of Cy5 was 633 nm, and the fluorescence signal with emission wavelength of 640 nm~740 nm was collected.

The cell imaging of color code the different amplification reaction in T24 cell. 2 mL of digested T24 cells were seeded in a cell petri dish. When the cell density grew to 70%, 200 μL of MnOx nanoprobes (the final concentration of MnOx nanoparticles was

80 μg·mL^{-1}, the final concentration of H1, H2, H3, H4-1, H5, H6-1(S-1, L-1) substrate hairpin probes was 100 nmol·L^{-1}) were added into the cell petri dish of T24 cells, and then 2 μL, 5 μmol·L^{-1} of DAPI staining reagent was added to each cell petri dish. The cell petri dish was incubated in the incubator for 6 h, then washed the petri dish with PBS for three times, washed off culture medium, and then used laser confocal microscope for fluorescence imaging of the cells. the excitation wavelength of DAPI was 405 nm, the excitation wavelength of DAPI was 410 nm~510 nm; the excitation wavelength of Cy5 was 633 nm; and the emission wavelength of Cy5 was 640 nm~740 nm; the excitation wavelength of Cy3 was 543 nm, and the emission wavelength of Cy3 was 550 nm~630 nm; the excitation wavelength of FAM was 488 nm, and the emission wavelength of FAM was 495 nm~540 nm.

Flow cytometry experiment

Firstly, 2 mL of digested T24 tumor cells and normal HCV29 cells were planted in 6-well plate (2 mL/well), respectively. When the cell density reached 70%, the culture medium in the well plate was discarded and then washed with PBS for three times. 2 mL of fresh culture fluid was added, and then 200 μL of PBS and 200 μL of MnOx-CHA nanoprobe (the final concentration of MnOx nanoparticles was 80 μg·mL^{-1}, the final concentration of H1, H2, H3 hairpin probe was 100 nmol·L^{-1}), 200 μL of MnOx-CHA-HCR nanoprobe (the final concentration of MnOx nanoparticles was 80 μg·mL^{-1}, H1, H2, H3, H4, H5 hairpin probe was 100 nmol·L^{-1}), 200 μL of MnOx-CHA-HCR-DNAzyme nanoprobe (the final concentration of MnOx nanoparticles was 80 μg·mL^{-1}, H1, H2, H3, H4, H4, H5, H6 substrate hairpin probe was 100 nmol·L^{-1}) were added to

the above two kinds of cells, respectively. The above resulting solution continued to incubate in 37 ℃ incubator for 12 h. The culture medium was discarded, washed with PBS for 3 times, digested with 100 μL of trypsin for 1 min. The cells were collected by 1200 rpm centrifugation for 5 min and passed through the membrane, and the cells were redispersed in 500 μL of PBS. The fluorescence intensity of Cy5 was detected by flow cytometry. The excitation wavelength of Cy5 was 633 nm.

For the flow experiment of down-regulating and up-regulating miRNA-21, the sample preparation process is as follows: first, 2 mL of T24 cells were cultured in a 6-well plate for 12 h, then liposome 3000 coated with miRNA-21i and miRNA-21 mimics was added, respectively, incubated in an incubator containing 5% CO2 at 37 ℃ for 24 h, and the culture medium was changed. 200 μL of MnOx-CHA-HCR-DNAzyme nanoprobe (the final concentration of MnOx nanoparticles was 80 $\mu g \cdot mL^{-1}$, H1, H2, H3, H4, H5, H6 substrate hairpin probe was 100 nmol L^{-1}) were added and continued to incubate for 12 h. The culture medium was discarded, washed with PBS for 3 times, digested with 100 μL of trypsin for 1 min, and centrifuged with 1200 rpm for 5 min to collect cells and cross the membrane. The cells were re-dispersed in 500 μL of PBS, and the fluorescence intensity of Cy5 was detected by flow cytometry. The excitation wavelength of Cy5 was 633 nm.

Quantitative reverse transcription-PCR (qRT-PCR) analysis of miRNA-21 in cell lysates

Total cellular RNAs were extracted from T24, HeLa, HepG2, HCV-29, 3T3 and 7702 cells using Trizol reagent (Sangon Co. Ltd., Shanghai, China) according to the

manufacturer's instructions. The cDNA samples were prepared by using the reverse transcription (RT) reaction with AMV First Strand cDNA Synthesis Kit. The cDNA samples were store at -20 °C for future use. qPCR analysis of cDNA was performed with SybrGreen PCR Master Mix (ABI, USA) on an ABI StepOnePlus qPCR instrument. The 20 μL reaction solution contained 2 μL cDNA sample, 10 μL of 2× SybrGreen qPCR Master Mix, 0.4 μL of 10 μM reverse primer, 0.4 μL of 10 μmol L^{-1} forward primer and 7.2 μL nuclease-free water. The PCR conditions were as follows: an initial 95 °C for 3 min followed by 40 cycles of 95 °C for 15 s, 57 °C for 20 s and 72 °C for 30 s.

Determination by MTT test

A group of normal cells (HCV-29 cells) and tumor cells (T24 cells) were used for toxicity analysis. Different material concentrations: 180 μL of digested HCV-29 cells and 180 μL of T24 cells were cultured in 96-well plate for 24 h, respectively, and 20 μL of MnOx nanoparticles with different concentrations were added to the 96-well plate, so that the final concentration of MnOx nanoparticles was 0, 10, 20, 40, 60, 80 $\mu g \cdot mL^{-1}$, respectively, and continued to culture for 24 h. Subsequently, 20 μL of MTT was added into the plate and continued incubating for 5-6 h. After that, the culture medium in the plate was discarded and added 100 μL of DMSO. The above obtained products were shaken at a low speed, and finally detected the absorbance of each well in the 96-well plate at the wavelength of 490 nm by using RT 6000 enzyme labeling instrument.

Results and discussion

Characterization of MnOx nanoparticles and MnOx nanoprobes

To verify the successful preparation of the MnOx nanoparticles, we used scanning electron microscope (SEM) to characterize the synthesized nanoparticles. As shown in Fig. S1A, the synthesized MnOx nanoparticles have a well-dispersed spherical structure, the particle size is uniform, and the average size is about 107 nm; the particle size of MnOx nanoprobes after DNA loading is 110 nm (Fig. S1B). The synthesized MnOx nanoparticles were characterized by dynamic light scattering (DLS). As shown in Fig. S1C, the average fluid diameter of MnOx nanoparticles is about 113 nm; the average fluid diameter of MnOx nanoprobes is about 118 nm (Fig. S1D). Compared with the SEM results, the particle size increases, which is caused by the hydration particle size measured in solution. As shown in Fig. S2, MnOx nanoparticles are positive charge. When DNA hairpin is modified on the surface of MnOx nanoparticles, MnOx nanoprobes exhibit negative charge, indicating that MnOx nanoprobes have been prepared successfully. To verify that there are different valence states of manganese in the MnOx nanoparticles, the MnOx nanoparticles were characterized by X-ray photoelectron spectroscopy (XPS). It can be seen from Fig. S3 that the manganese element of MnOx nanoparticles is composed of Mn^{II}, Mn^{III} and Mn^{IV}. The ratio of three different valence states is 1：3.46：2.99.

Release of Mn^{2+} under different GSH concentrations

To investigate the release of Mn^{2+} from MnOx nanoprobes in different concentrations of GSH, MnOx nanoprobes were incubated in buffers solution with

GSH concentrations of 0, 0.4, 0.8, 1.2, 1.6 and 2.0 mmol·L^{-1} for 6 h, respectively, and the concentration of Mn^{2+} was determined by ICP-MS. The experimental results are shown in Fig. S4. When the pH is 5.5 and incubation time is 6 h, the concentration of Mn^{2+} increases gradually with the increase of GSH concentration. When the concentration of GSH is 2.0 mmol L^{-1} (the concentration of GSH in tumor cells is about 2.0 mmol·L^{-1}), the concentration of Mn^{2+} in the solution is about 1.2 mmol·L^{-1}, which reaches the ion concentration required by DNAzyme cleavage reaction. The above experimental results show that MnOx nanoprobes can be degraded by GSH and release Mn^{2+}. The released Mn^{2+} is used as a cofactor of DNAzyme cleavage reaction in the simulating tumor cell intracellular environment with pH 5.5 buffer solution and 6 h incubation time.

Fluorescence detection of DNAzyme activation in vitro

Whether DNAzyme is activated or not directly affects the model amplification efficiency of the sensing system. Under different conditions, the cleavage of the substrate by DNAzyme was verified by detecting the fluorescence intensity of the substrate strand (Fig. S5). the substrate strands were labeled with FAM and DABCYL, respectively. Only in the presence of miRNA-21 and Mn^{2+}, the fluorescence of the substrate chain was significantly enhanced. This proves that the DNAzyme can cleave the substrate only in the presence of miRNA-21 and Mn^{2+}.

Experimental characterization of gel electrophoresis

To verify the feasibility of the CHA-HCR-DNAzyme sensing system, we used polyacrylamide gel electrophoresis to investigate. As shown in Fig. S6. Channel 1 is H1, channel 2 is H2, channel 3 is H3, channel 10 is H4, channel 11 is H5, there is only one obvious band, respectively. channel 9 is the band of the target miRNA-21, because the target DNA base number is less, so it is not shown in channel 9. Channel 4, channel 5, channel 12 and channel 13 are H1/H2, H1/H2/H3, H4/H5 and H1/H2/H3/H4/H5/H6 respectively, and only their corresponding obvious bands appear, which indicates that these DNA hairpins can exist stably without target miRNA-21 and there is no hybridization reaction. Channel 6 is a mixture of miRNA21/H1, and a band that moves more slowly than channel 1 appears in channel 6, which is due to the formation of a complex miRNA-21-H1 with a larger molecular weight than H1 under the action of the target miRNA-21. Channel 7 is a mixture of miRNA-21/H1/H2, and a band that moves more slowly than channel 6 appears in channel 7, which indicates that the miRNA-21-H1 complex opens the H2 hairpin to form a complex miRNA-21-H1-H2 with a molecular weight higher than that of miRNA-21-H1. Channel 8 is a mixture of miRNA-21/H1/H2/H3, and a band that moves more slowly than channel 7 appears in channel 8, which indicates that the miRNA-21-H1-H2 complex opens the H3 hairpin to form a complex miRNA-21-H1-H2-H3 with a molecular weight higher than miRNA-21-H1-H2 and a new bands similar to miRNA-21. Therefore, the CHA reaction takes place, and the Y-type DNA double-strand structure is formed by cyclic self-assembly. Channel 14 is a mixture of miRNA21/H1/H2/H3/H4, and a band that moves slowly relative to channel 10 appears in channel 14 and. This result indicates that the miRNA-

21-H1-H2-H3 complex opens the hairpin H4 to form a complex miRNA-21-H1-H2-H3-H4 with a molecular weight higher than that of miRNA-21-H1H2-H3. Channel 15 is a mixture of miRNA21/H1/H2/H3/H4/H5, and a continuous band appears in channel 15, which indicates that the miRNA21-H1-H2-H3-H4 complex opens the hairpin H5, and the HCR reaction occurs. Namely, the continuous band appears in accordance with the characteristics of the HCR reaction. Channel 18 is a mixture of miRNA-21/H1/H2/H3/H4/H5/H6, and there is also a continuous band of HCR in channel 15. Additionally, a band at the same position as channel 19 appears below, which is a single strand L dropped from DNAzyme after cleaving the substrate, corresponding to the L of channel 19. It indicates that the cleavage effect of DNAzyme has been reflected. The above channel band results are consistent with the feasibility verification results of spectral experiments.

The influence of reaction time

In the experiment, the reaction time is closely related to the fluorescence amplification efficiency of the reaction system. If the reaction time is too long, the experimental time will be wasted, and the amplification efficiency of the system will not be reflected. Therefore, to obtain the optimal reaction time for the specific binding of the CHA-HCR-DNAzyme sensing system with tumor marker miRNA-21, 0.5 nmol L^{-1} of target miRNA-21 and 6 hairpin DNA were incubated for different time, and carried out fluorescence detection. As shown in Fig. S7, when the reaction time increases, the fluorescence intensity of Cy5 increases, and when the reaction time

exceeds 150 min, the fluorescence signal intensity of Cy5 does not change significantly. So, 150 min was selected as the optimal reaction time to detect the target in the solution system.

Fluorescence detection of miRNA-21

To investigate the detection performance of the CHA-HCR-DNAzyme sensor system for miRNA-21, fluorescence detection of a series of miRNA-21 with different concentrations was carried out under the above optimized conditions. Fig. S8 shows the experimental results. When the CHA-HCR-DNAzyme sensor system is adopted, the fluorescence of Cy5 gradually increases with the increase of miRNA-21 concentration (Fig. S8A-B). This is because the increase of miRNA-21 concentration can trigger more CHA-HCR-DNAzyme cycle cleavage amplification reaction, so that more H1 and H4 hairpins labeled with Cy5 fluorophores are opened and fluorescence recovery is achieved. Linear regression analysis of the logarithmic value of miRNA-21 concentration by Cy5 fluorescence intensity showed that the miRNA-21 concentration showed a good linear relationship at 20 amol·L^{-1}~5 pmol·L^{-1}. The linear equation was FL= 33.91LgC + 80.21, R^2= 0.993. FL was fluorescence intensity of Cy5 at 665 nm, and C was miRNA-21 concentration value. According to the 3σ method, the detection limit of the sensor system for miRNA-21 was 13 amol·L^{-1}. To better reflect the powerful detection function of the CHA-HCR-DNAzyme sensor system, CHA sensor system and CHA-HCR sensor system were used to measure a series of miRNA-21 with different concentrations under the same experimental conditions, and compared the results with the experimental results of CHA-HCR-DNAzyme sensor system. When the

CHA-HCR sensor system was used to detect miRNA-21, the linear range of miRNA-21 was 30 fmol/L~ 1 nmol /L, and the detection limit was 17 fmol·L^{-1} (Fig. S8C-D), which was 3 orders of magnitude lower than the detection limit of CHA sensor system. But the detection limit was at least 3 orders of magnitude higher than that of CHA-HCR-DNAzyme sensor system. When CHA sensor system was used to detect miRNA-21, the linear range of miRNA-21 was 50 pmol·L^{-1}~300 nmol·L^{-1}, and the detection limit was 27 pmol·L^{-1} (Fig. S8E-F), which was at least 6 orders of magnitude higher than the detection limit of CHA-HCR-DNAzyme sensor system. The above experimental results showed that the CHA-HCR-DNAzyme sensor system had stronger signal amplification capability and higher detection sensitivity due to the introduction of CHA, HCR and DNAzyme amplification response strategies. This method was compared with the previously reported miRNA sensing system[2-5] based on different nanomaterials and different amplification strategies. The results are shown in Table S2. The nucleic acid biosensor has high detection sensitivity.

Specificity test

To investigate the selectivity of the constructed cyclic amplification sensing method for miRNA-21 detection, the above three different sensing systems were used for fluorescence determination of target miRNA-21, other endogenous miRNA (miRNA-223, miRNA-219 and miRNA-141) and corresponding mixtures with the same concentration (0.5 nmol·L^{-1}). The experimental results were shown in Fig. S9. When the target miRNA-21 was introduced into the CHA sensor system, CHA-HCR sensor system and CHA-HCR-DNAzyme sensor system, the fluorescence intensity of the

above sensor systems was increased. Under the same experimental conditions, when other endogenous miRNA with the same concentration was added into three sensor systems, the fluorescence intensity of the systems did not change significantly compared with that of the control group. When the mixtures containing target miRNA-21 and other endogenous miRNA were added into the sensor systems, the fluorescence intensity of the system was almost similar with the sensor systems which were added miRNA-21 alone, and the fluorescence signal of the CHA-HCR-DNAzyme sensor system increased significantly. The above experimental results showed that the three different sensing systems had good response specificity to miRNA-21.

Effect of incubation time on Cy5 fluorescence imaging in T24 cells

The incubation time of the CHA-HCR-DNAzyme nanoprobes in cells can affect Mn^{2+} release and the binding degree of hairpin DNA to target miRNA-21. Therefore, T24 cells and nanoprobes were incubated for different periods (3, 4, 5, 6 and 7 h), and fluorescence imaging was performed under laser confocal microscope and explored the best incubation time. Results as shown in Fig. S10, the fluorescence signal of Cy5 in cells can be seen at 3 h of incubation time, and the fluorescence intensity increases gradually with the increase of incubation time. This was because the CHA-HCR-DNAzyme nanoprobes begin to degrade to release Mn^{2+} under the action of intracellular GSH. Meanwhile, DNA hairpins were gradually released and specifically bound with the target miRNA-21. Subsequently, CHA, HCR and DNAzyme reactions occurred, and Cy5 fluorescence recovered. When the incubation time was at 6 h, a strong fluorescence signal could be observed, and then the fluorescence signal did not change

significantly with the increase of incubation time, indicating that the release of DNA hairpin and the binding with the target mirNA-21 had reached a balance after the nanoprobes entered the cell. Therefore, 6 h was selected as the best incubation time for the nanoprobes and used for subsequent cell experiments.

The cell imaging of color code the different amplification reaction in T24 cell.

To ensure three the amplification reaction happen in the same region, colour coding experiments for intracellular amplification reactions have been performed. As shown in Fig. S11, the colors representing the three amplification reactions almost overlap in the cytoplasm (Fig. S11A), CHA/HCR amplification reaction with a colocalization coefficient of 0.926, CHA/DNAzyme amplification reaction with a colocalization coefficient of 0.904, HCR/DNAzyme amplification reactions with a colocalization coefficient of 0.914 (Fig. S11B). Illustration of color code the three amplification reactions (Fig. S11C). Cy5 fluorescence was observed during CHA reaction. Cy3 fluorescence was observed during HCR reaction. FAM fluorescence was observed during DNAzyme reaction. This proves that all three amplification reactions can happen with the same efficiency in the same miRNA-21.

Different nanoprobes for fluorescence imaging analysis of miRNA-21 in different cell lines

To investigate that the MnOx nanoprobes can be used for signal amplification imaging analysis of intracellular target miRNA-21, four different sensing systems were

incubated with three different tumor cells and three corresponding normal cells for the same incubation time for cell fluorescence imaging. As shown in Fig. 2, Fig. S12 and Fig. S14, MnOx-H1 nanoprobe, MnOx-CHA nanoprobe, MnOx-CHA-HCR nanoprobe and MnOx-CHA-HCR-DNAzyme nanoprobe all has obvious fluorescence to the three tumor cells, but the three normal cells almost no fluorescence was observed. The response signals of the four sensor systems to the target miRNA-21 were MnOx-CHA-HCR-DNAzyme nanoprobe, MnOx-CHA-HCR nanoprobe, MnOx-CHA nanoprobe and MnOx-H1 nanoprobe in descending order. These results further confirmed that MnOx nanoprobes could be used for ultrasensitive imaging of miRNA-21 in tumor cells, which was consistent with the conclusion obtained in solution system, and could be used to distinguish normal cells from tumor cells. Similar results were obtained by detecting the fluorescence intensity of different cells with different sensing systems (Fig. S13 and Fig. S15).

Determination of miRNA-21 in cell lysates with the proposed method and RT-PCR

In order to establish a reliable result from the assay, the expression level of miRNA-21 from different cell lines was detected using the proposed method and RT-PCR (Fig. S16 A). In addition, different concentrations of miRNA-21 in T24 cell lysates were also detected by the proposed method and RT-PCR (Fig. S16 B). It can be seen from the experimental results that the results obtained by the proposed method are similar to PCR and have a good correlation. This result proves that the proposed release method can be used to quantify miRNA-21 in cell lysates.

Imaging analysis of down-regulated and up-regulated miRNA-21 in cells

To further confirm that the signal output of the MnOx-CHA-HCR-DNAzyme nanoprobe was related to the expression level of miRNA-21 in cells, we added MnOx-CHA-HCR-DNAzyme nanoprobe into the T24 cells treated with miRNA-21i and miRNA-21 mimics for cell imaging analysis. It can be seen from Fig. S17 that the Cy5 fluorescence intensity of T24 cells treated with miRNA-21i is weakened, treated with miRNA-21 mimics is enhanced. The miRNA-21 expression level of T24 is up treated with miRNA-21 mimics. The lower the miRNA-21 expression level, the number of MnOx-CHA-HCR-DNAzyme nanoprobe activated by targets also decreased, and the fluorescence intensity was significantly weaker than that of untreated cells. The higher the miRNA-21 expression level, the number of MnOx-CHA-HCR-DNAzyme nanoprobe activated by targets also increased, and the fluorescence intensity was significantly enhanced than that of untreated cells. The above experiments proved that the fluorescence signal output of MnOx-CHA-HCR-DNAzyme nanoprobe was related to the expression level of miRNA-21 in cells, namely, it had good specificity.

Flow cytometric analysis of miRNA-21 in cells

To verify that the signal output of the MnOx-CHA-HCR-DNAzyme nanoprobe was related to the expression level of miRNA-21 in cells, MnOx-CHA-HCR-DNAzyme nanoprobe were added into T24 cells pretreated with miRNA-21i and miRNA-21 mimics for flow cytometric analysis. It can be seen from the Fig. S18 that the Cy5 fluorescence intensity of T24 cells pretreated with miRNA-21i is weakened, which is

because lower expression level of miRNA-21 and less MnOx-CHA-HCR-DNAzyme nanoprobe activated by the target miRNA-21, and the fluorescence intensity is significantly lower than that of untreated cells. The Cy5 fluorescence intensity of T24 cells pretreated with miRNA-21 mimics is enhanced, which is due to higher the miRNA-21 expression level and more MnOx-CHA-HCR-DNAzyme nanoprobes activated by the target, and the fluorescence intensity is significantly enhanced than that of untreated cells. Similar results were obtained by RT-PCR (Fig. S19). These results revealed that the developed nanoprobe was able to give fluorescence signals dynamically correlated to the expression level of the target miRNA-21, further confirming that the developed nanoprobe had the potential for quantifying miRNA expression in living cells.

To further verify that the MnOx nanoprobes can achieve intracellular miRNA-21 signal amplification analysis, tumor cells T24 and normal cells HCV-29 were taken as models. Flow cytometry was used to detect Cy5 fluorescence of cells after transfection with MnOx-CHA nanoprobes, MnOx-CHA-HCR nanoprobes and MnOx-CHA-HCR-DNAzyme nanoprobes, respectively. The experimental results showed that when Cy5 fluorescence was used for analysis, the fluorescence intensity of tumor cells transfected with MnOx-CHA-HCR-DNAzyme nanoprobes was the highest, followed by that of MnOx-CHA-HCR nanoprobes. The fluorescence intensity of tumor cells after transfection with MnOx-CHA nanoprobes was the lowest, but all of them were stronger than Cy5 fluorescence intensity obtained by analyzing normal cells (Fig. S20). The results obtained by flow fluorescence analysis were consistent with those obtained by confocal laser microscopy, which proved that the MnOx nanoprobes could be used for

intracellular miRNA-21 signal amplification analysis and could distinguish tumor cells from normal cells.

Biocompatibility test

To investigate the biocompatibility of MnOx nanoparticles, standard 3-(4, 5-dimethylthiazole-2-yl) -2, 5-diphenyltetrazolium bromide (MTT) test was used for analysis. As shown in Fig. S21, after incubation for 24 h, the survival rate of both T24 tumor cells and HCV29 normal cells exceeds 95% in the concentration range of 0-80 $\mu g \cdot mL^{-1}$ of MnOx nanoparticles. This result indicates that MnOx nanoparticles have good biocompatibility and almost negligible cytotoxicity. Therefore, 80 $\mu g \cdot mL^{-1}$ of MnOx nanoparticles was selected as the optimal concentration for the experiment.

Reference:

[1] H. L. Yu, L. Zheng, *Microchim. Acta*., 2016, **183**, 2229-2234.

[2] L. Yang, Q. Wu, Y. Q. Chen, X. Q. Liu, F. A. Wang and X. Zhou, *ACS Sens.*, 2019, **4**, 110-117.

[3] D. G. He, X. He, X. Yang and H.-W. Li, *Chem. Sci*., 2017, **8**, 2832-2840.

[4] H. Wang, H. M. Wang, Q. Wu, M. J. Liang, X. Q. Liu and F. A. Wang, *Chem. Sci*., 2019, **10**, 9597-9604.

[5] J. Wei, H. M. Wang, Q. Wu, X. Gong, K. Ma, X. Q. Liu and F. A. Wang, Angew. Chem., Int. Ed., 2020, 132, 6021-6027.

Supporting figures

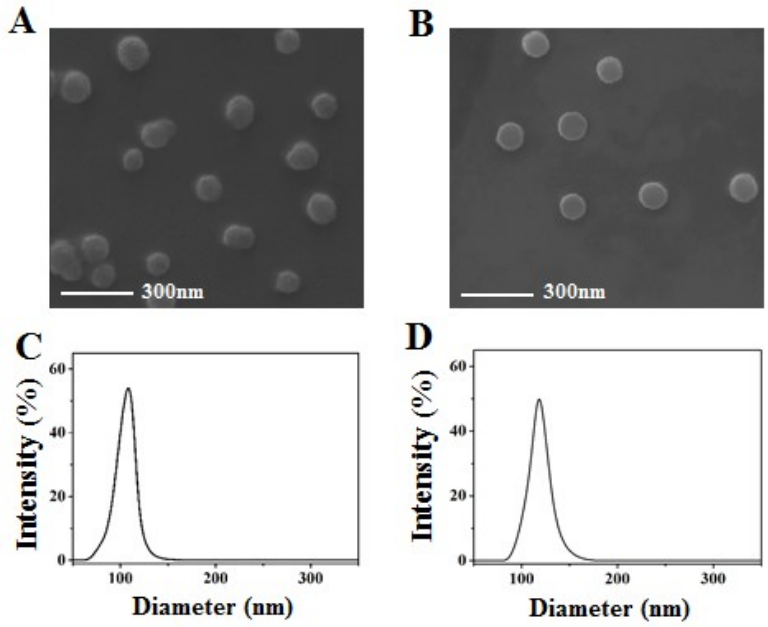

Fig. S1 SEM of MnOx nanoparticles (A); SEM of MnO_X-CHA-HCR-DNAzyme nanoprobe (B); DLS of MnOx nanoparticles (C); DLS of MnOX-CHA-HCR-DNAzyme nanoprobe (D).

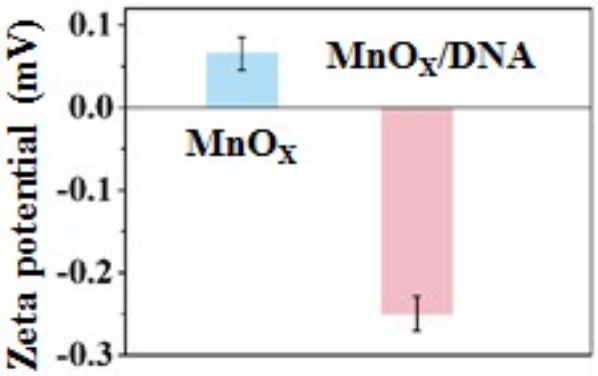

Fig. S2 Zeta potential characterization diagram of MnOx nanoparticles and MnOx nanoprobes. Error bars were derived from N=5 experiments.

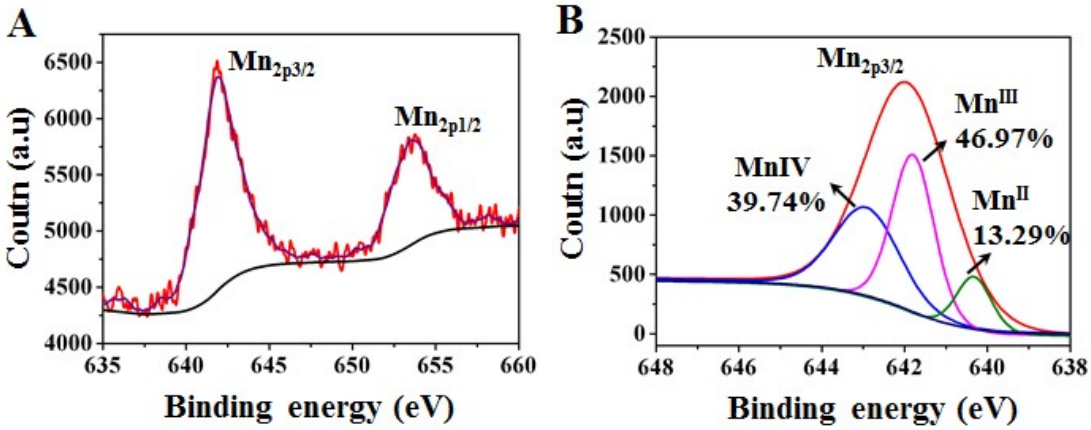

Fig. S3 Characterization of MnOx nanoparticles by X-ray photoelectron spectroscopy (XPS).

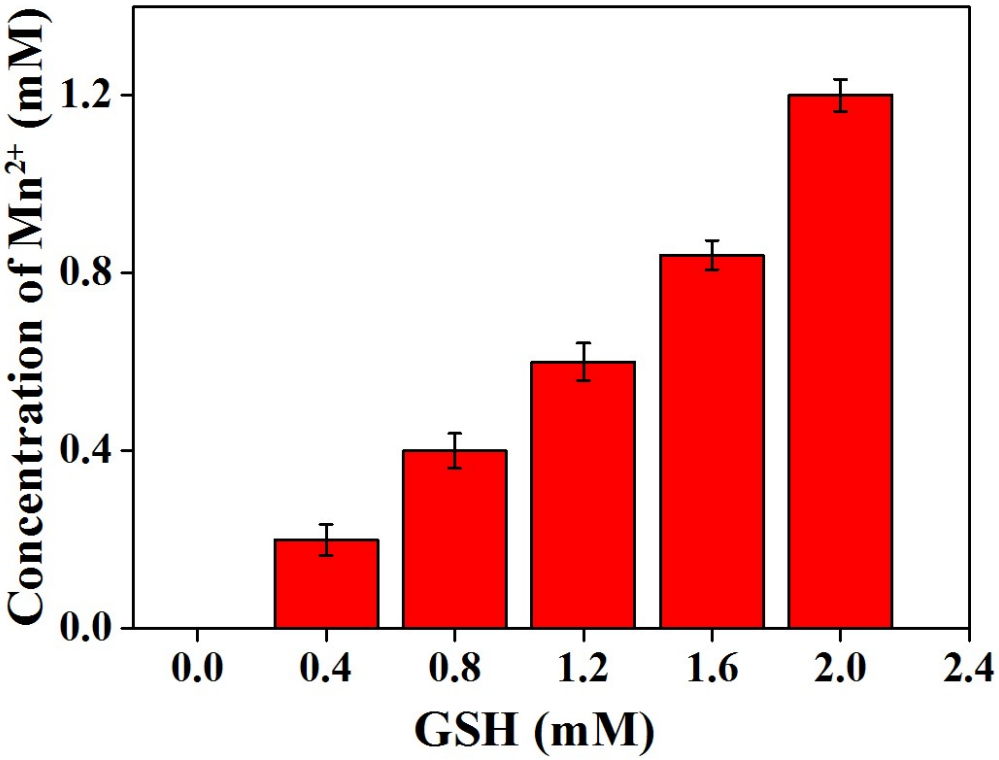

Fig. S4 The release of Mn^{2+} under different GSH concentrations. Error bars were derived from N=5 experiments.

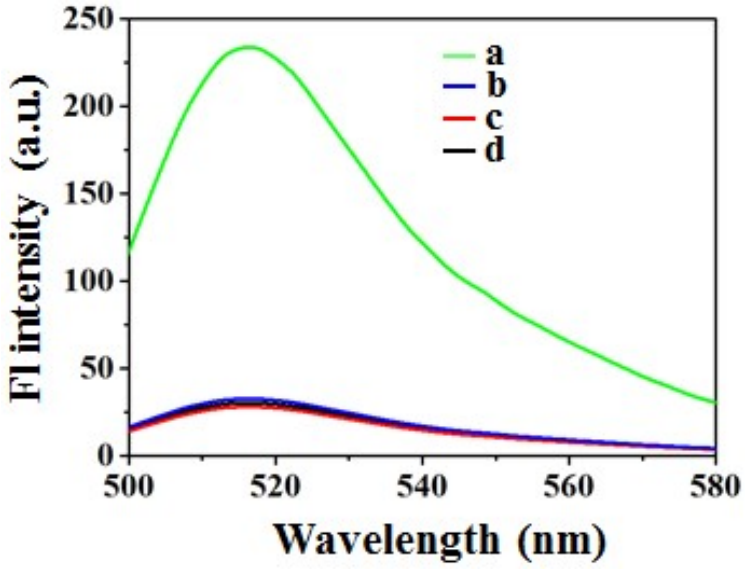

Fig. S5 Fluorescence spectra of DNAzyme substrate strand. a: CHA-HCR-DNAzyme sensing system, miRNA-21 and 5 mmol L^{-1} Mn^{2+}; b: CHA-HCR-DNAzyme sensing system, miRNA-21; c: CHA-HCR-DNAzyme sensing system and 5 mmol L^{-1} Mn^{2+}; d: CHA-HCR-DNAzyme sensing system.

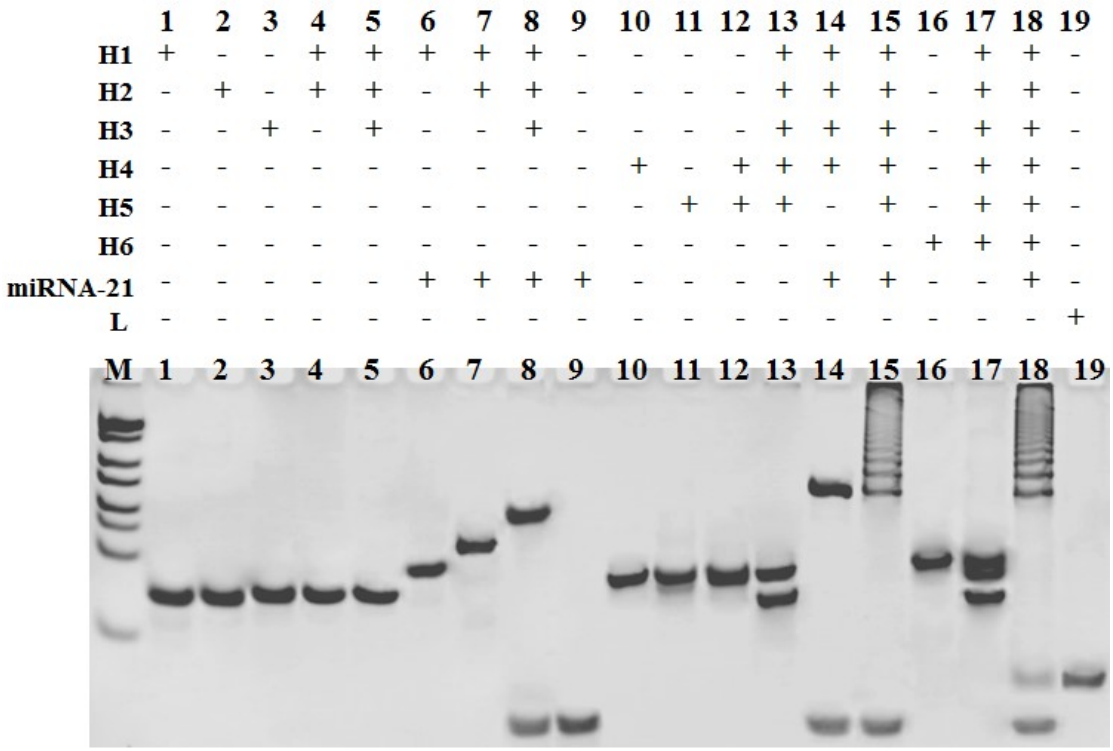

Fig. S6 Gel electrophoresis characterization of miRNA-21. 1: H1; 2: H2; 3: H3; 4: H1/H2; 5: H1/H2/H3; 6: miRNA-21/H1; 7: miRNA-21/H1/H2; 8: miRNA-21/H1/H2/H3; 9: miRNA-21; 10: H4; 11: H5; 12: H4/H5; 13: H1/H2/H3/H4/H5; 14: miRNA-21/H1/H2/H3/H4; 15: miRNA-21/H1/H2/H3/H4/H5; 16：H6; 17: H1/H2/H3/H4/H5/H6; 18: miRNA-21/H1/H2/H3/H4/H5/H6; 19: L; Each sample for gel electrophoresis analysis contained 5 mM Mn^{2+}.

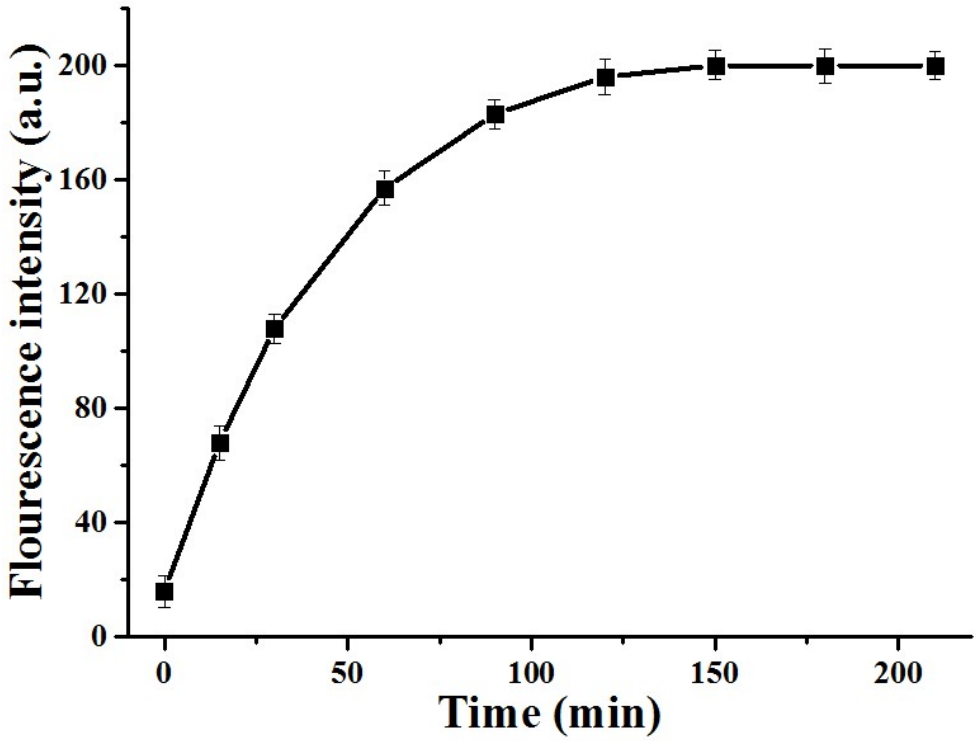

Fig. S7 The effect of different reaction time on miRNA-21 detection (the final concentration of miRNA-21 is 0.5 nmol·L^{-1}, the reaction time is 0 min, 15 min, 30 min, 60 min, 90 min, 120 min, 150 min, 180 min, 210 min; Cy5 excitation wavelength is 633 nm, emission wavelength is 660 nm, excitation and emission gap width is 10 nm, voltage is 700 V). All samples contained 5 mmol L^{-1} Mn^{2+}. Error bars were derived from N=5 experiments.

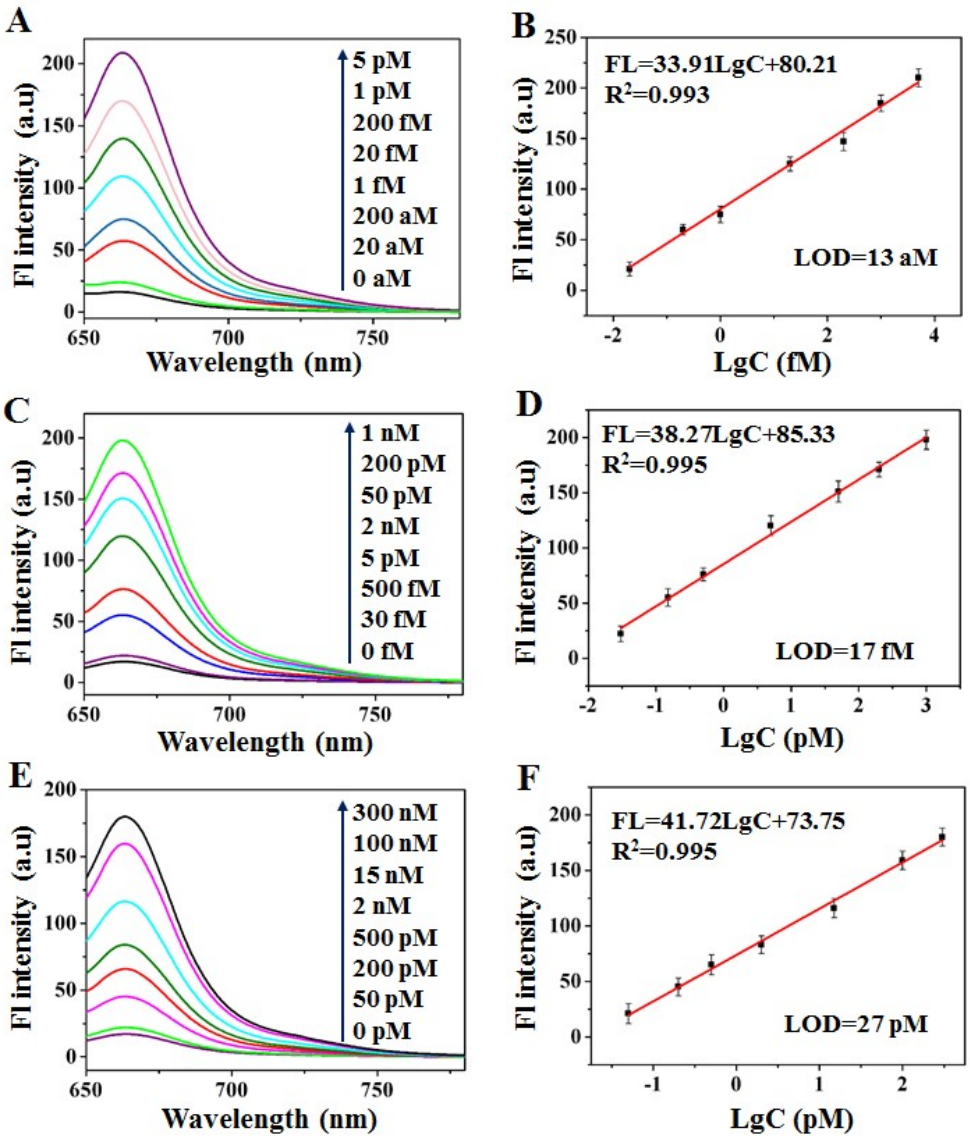

Fig. S8 Fluorescence spectra of the proposed CHA-HCR-DNAzyme sensing systems upon the detection of TK1 mRNA at different concentrations (A). Calibration curves corresponding to the proposed CHA-HCR-DNAzyme sensing systems (B). Fluorescence spectra of the proposed CHA-HCR sensing systems upon the detection of TK1 mRNA at different concentrations (C). Calibration curves corresponding to the proposed CHA-HCR sensing systems (D). Fluorescence spectra of the proposed CHA sensing systems upon the detection of TK1 mRNA at different concentrations (E). Calibration curves corresponding to the proposed CHA sensing systems (F). All samples contained 5 mmol L^{-1} Mn^{2+}. Error bars were derived from N=5 experiments.

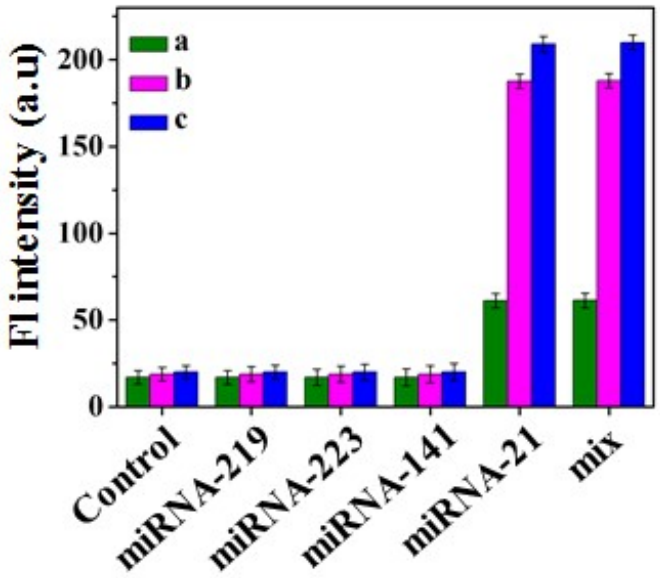

Fig. S9 Specificity response of different sensing systems to different targets (same concentration) (a: CHA sensing system; b: CHA-HCR sensing system; c: CHA-HCR-DNAzyme sensing system). All samples contained 5 mmol L^{-1} Mn^{2+}. Error bars were derived from N=5 experiments.

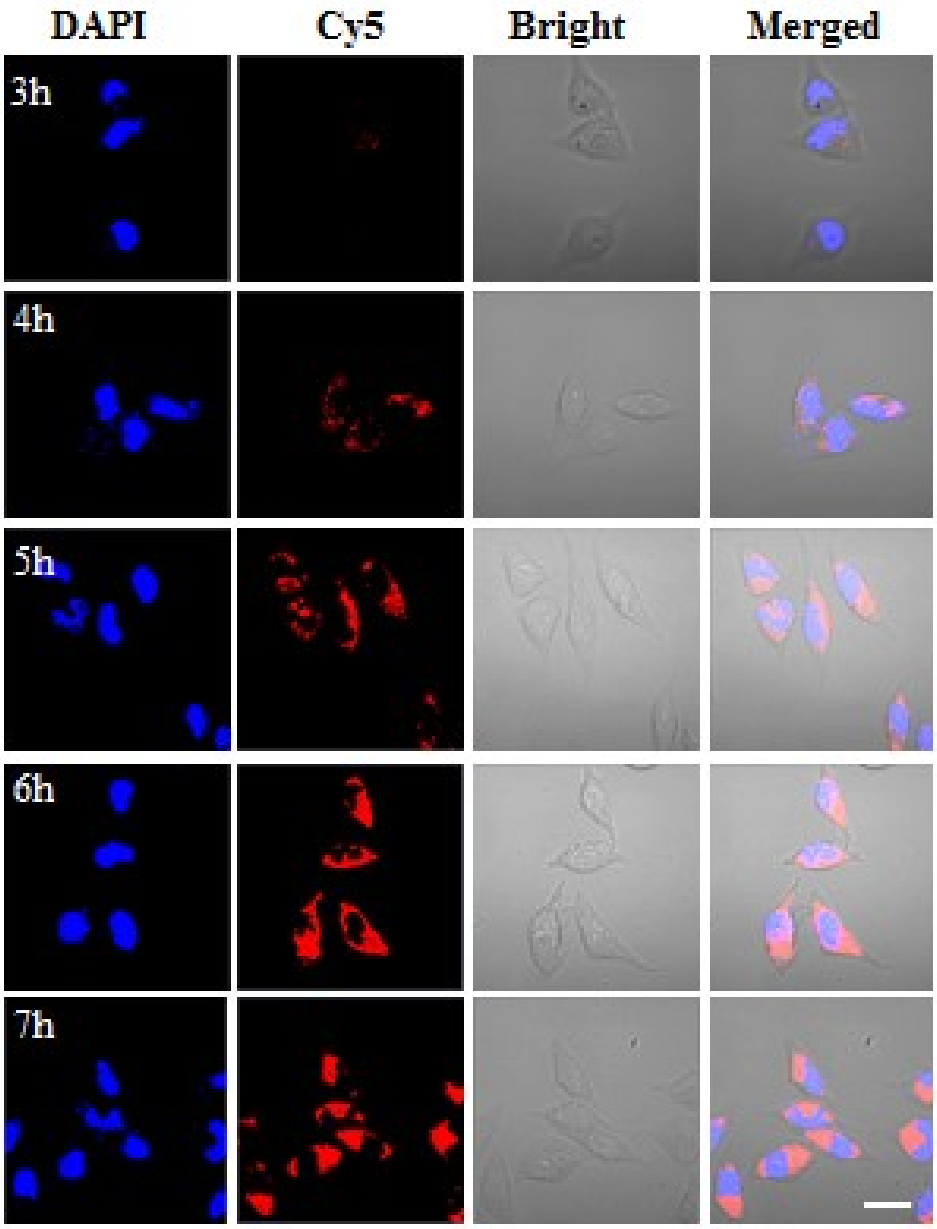

Fig. S10 The fluorescence images of MnOx-CHA-HCR-DNAzyme nanoprobes incubated in T24 cells for different times (the final concentration of MnOx-CHA-HCR-DNAzyme nanoprobe was 80 μg mL^{-1}, the excitation wavelength of DAPI was 405 nm, the excitation wavelength of DAPI was 410 nm~510 nm, the excitation wavelength of Cy5 was 633 nm, and the emission wavelength of Cy5 was 640 nm~740 nm). Scale bar = 20 μm.

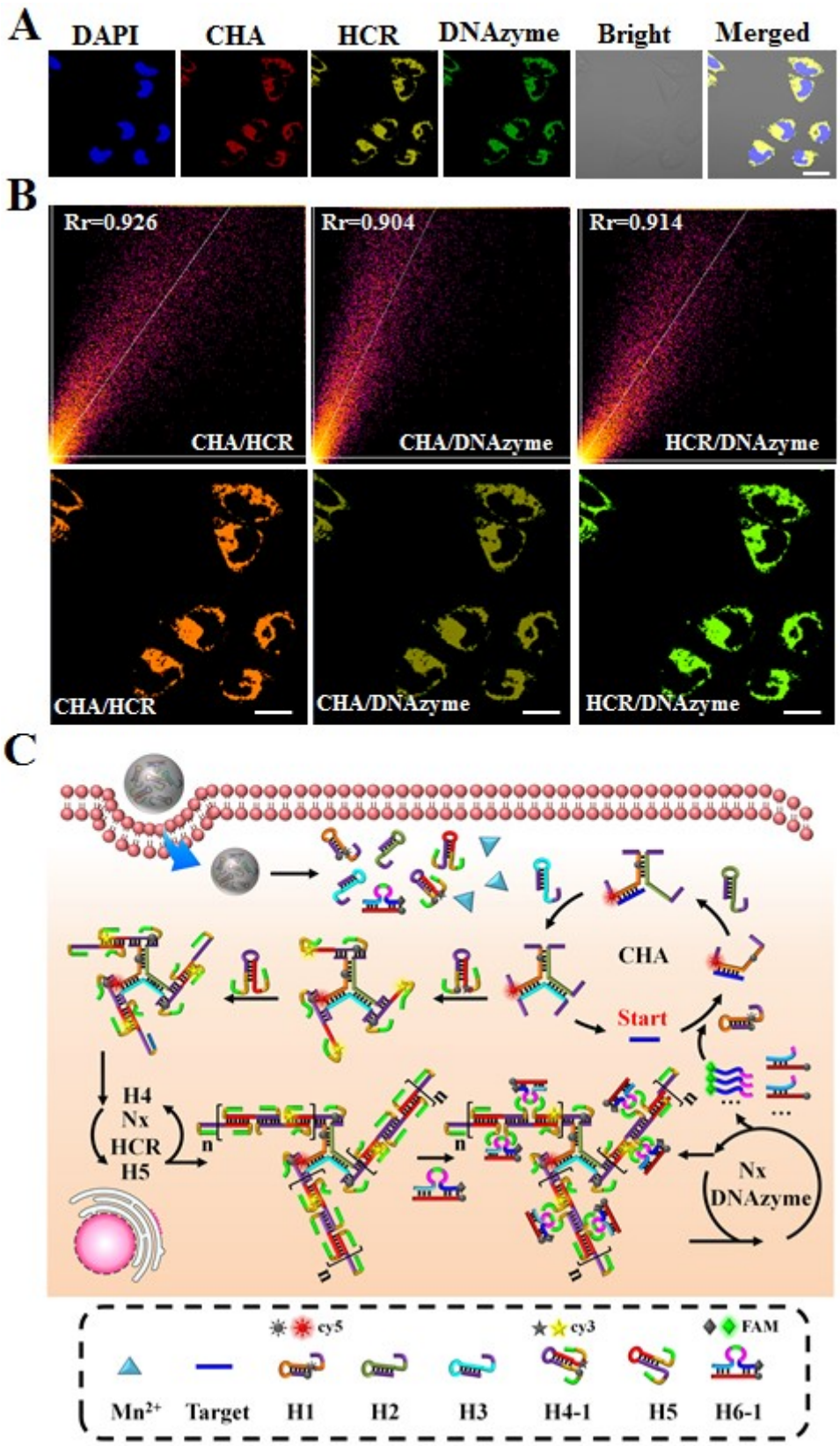

Fig. S11 (A) The fluorescence images of MnOx-CHA-HCR-DNAzyme nanoprobes incubated in T24 cells at 6h (the final concentration of MnOx-CHA-HCR-DNAzyme

nanoprobe was 80 μg mL^{-1} ; the final concentration of H1, H2, H3, H4-1, H5, H6-1(S-1, L-1) were 100 nmol L^{-1}, respectively; the excitation wavelength of DAPI was 405 nm, the excitation wavelength of DAPI was 410 nm~510 nm; the excitation wavelength of Cy5 was 633 nm; the excitation wavelength of Cy3 was 543 nm, and the emission wavelength of Cy3 was 550 nm~620 nm; the excitation wavelength of FAM was 488 nm, and the emission wavelength of FAM was 495 nm~540 nm; nm). (B) Colocalization images of the different amplification reactions. (C) Illustration of color code the three amplification reactions. Scale bar = 20 μm.

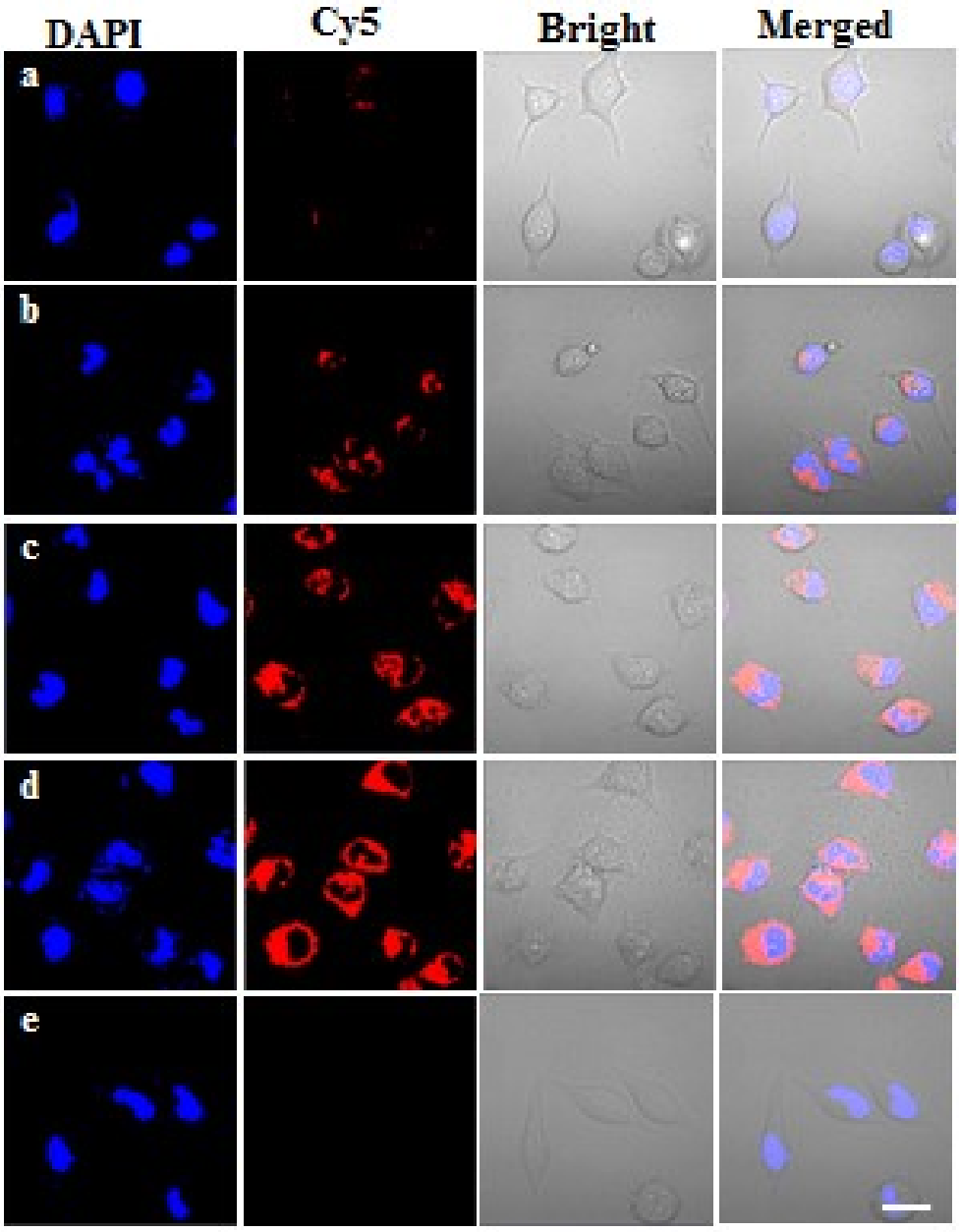

Fig. S12 miRNA-21 imaging analysis of different systems in different cell lines: MnO_X-H1 sensing system in HepG-2 cells (a); MnO_X-CHA nanoprobe in HepG-2 cells (b); MnO_X-CHA-HCR nanoprobe in HepG-2 cells (c); MnO_X-CHA-HCR-DNAzyme nanoprobe in HepG-2 cells (d); MnO_X-CHA-HCR-DNAzyme nanoprobe in HL-7702 cells (e). Scale bar = 20 μm.

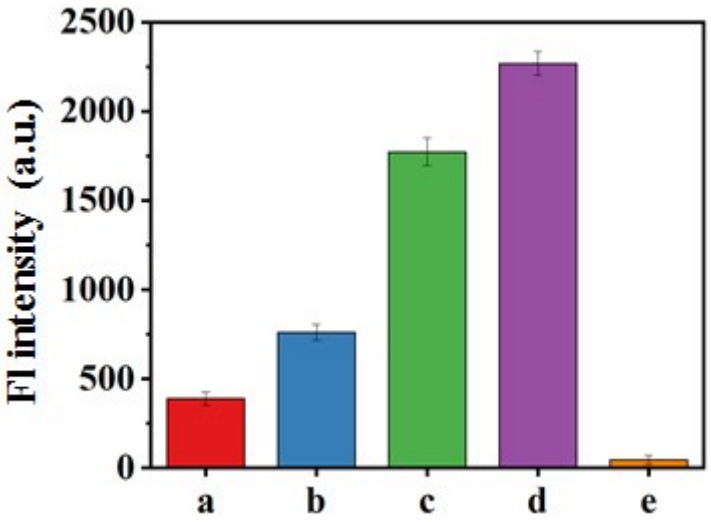

Fig. S13 Fluorescence intensity of different systems in different cell lines: MnO_X-H1 sensing system in HepG-2 cells (a); MnO_X-CHA nanoprobe in HepG-2 cells (b); MnO_X-CHA-HCR nanoprobe in HepG-2 cells (c); MnO_X-CHA-HCR-DNAzyme nanoprobe in HepG-2 cells (d); MnO_X-CHA-HCR-DNAzyme nanoprobe in HL-7702 cells (e). Error bars were derived from N=5 experiments.

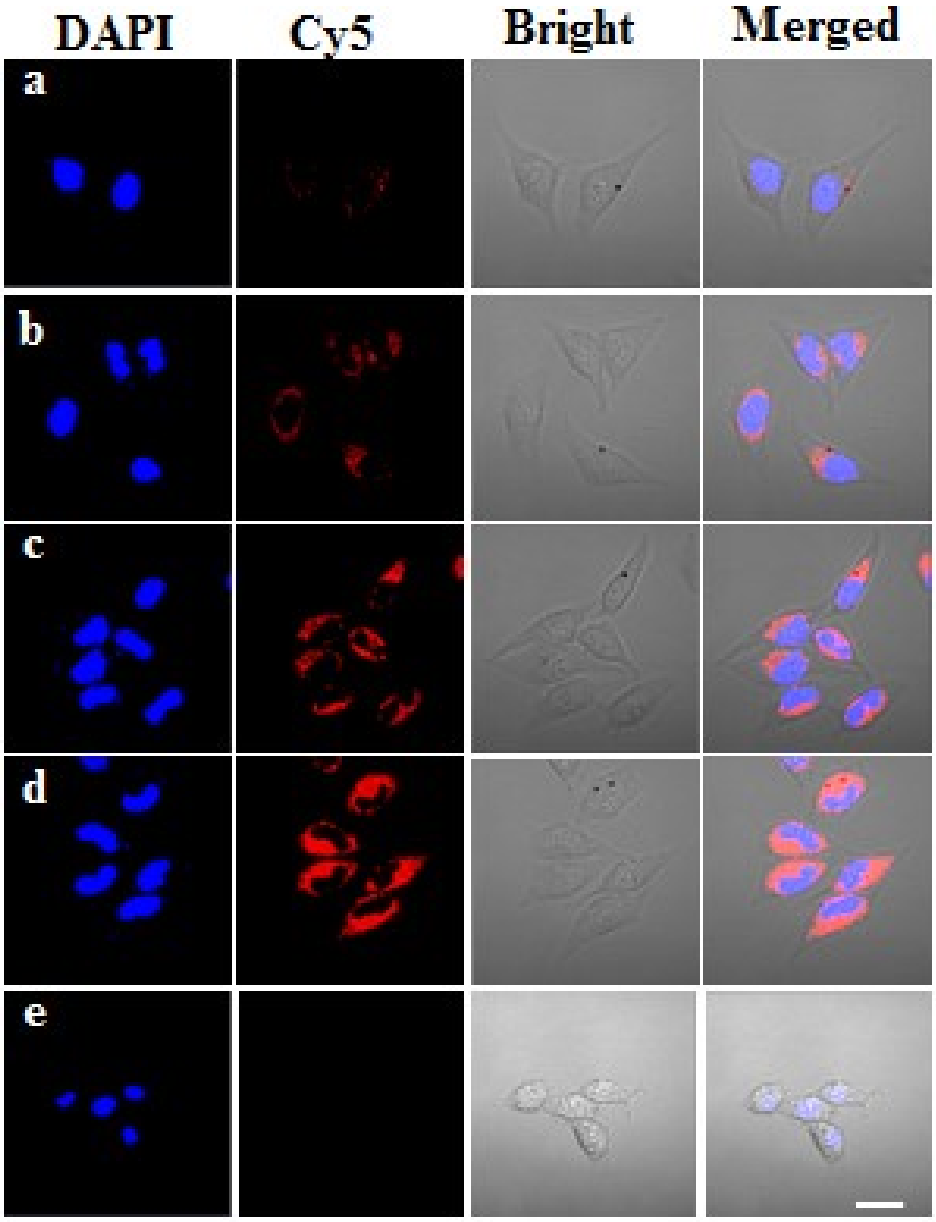

Fig. S14 miRNA-21 imaging analysis of different systems in different cell lines: MnOx-H1 sensing system in HeLa cells (a); MnOx-CHA nannoprobe in HeLa cells (b); MnOx-CHA-HCR nanoprobe in HeLa cells (c); MnOx-CHA-HCR-DNAzyme nanoprobe in HeLa cells (d); MnOx-CHA-HCR-DNAzyme nanoprobe in 3T3 cells (e). Scale bar = 20 μm.

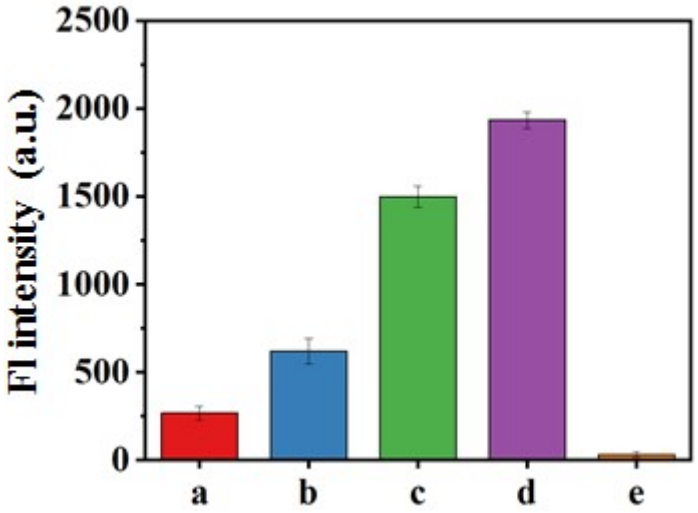

Fig. S15 Fluorescence intensity of different systems in different cell lines: MnOx-H1 sensing system in HeLa cells (a); MnOx-CHA nannoprobe in HeLa cells (b); MnOx-CHA-HCR nanoprobe in HeLa cells (c); MnOx-CHA-HCR-DNAzyme nanoprobe in HeLa cells (d); MnOx-CHA-HCR-DNAzyme nanoprobe in 3T3 cells (e). Error bars were derived from N=5 experiments.

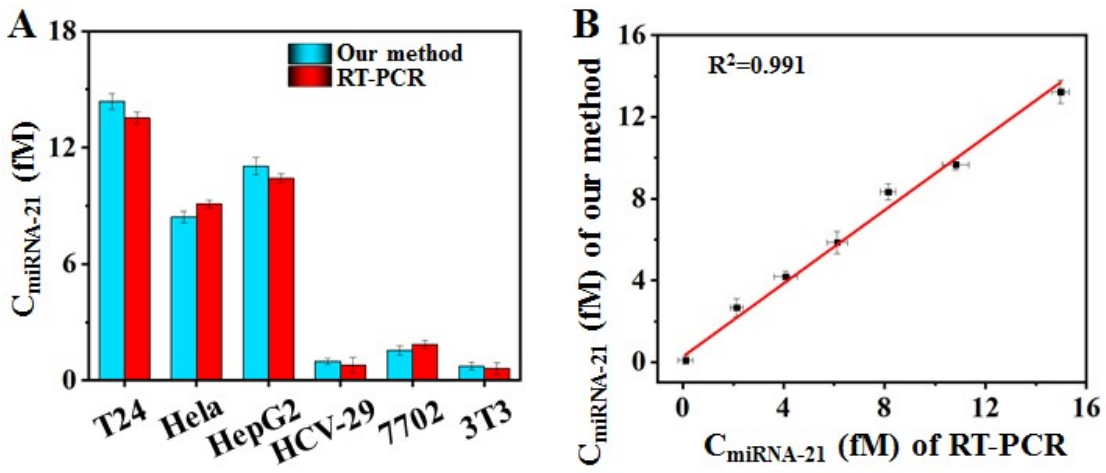

Fig. S16 (A) Real sample analysis of miRNA-21 detection in different cell lysates. (B) Real sample analysis of miRNA-21 detection in different concentration T24 cell lysates correlation curve. The RT-PCR value is obtained by dividing the detection value of the instrument by 1000 (CRT-PCR=C0/1000). All samples contained 5 mmol L^{-1} Mn^{2+}. Error bars were derived from N=5 experiments.

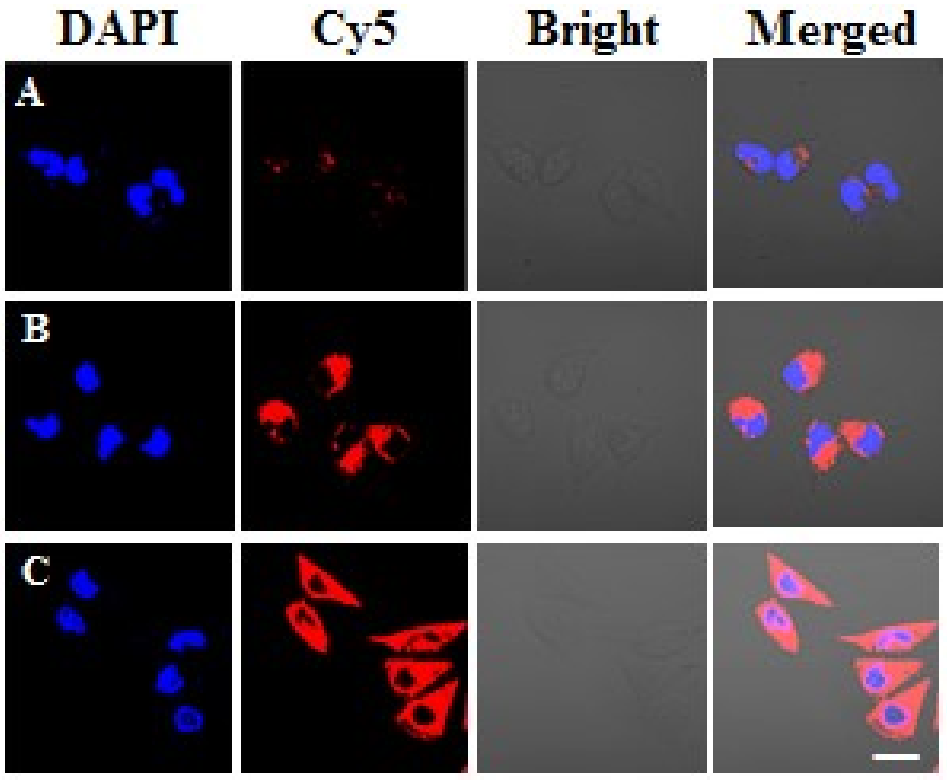

Fig. S17 miRNA-21 down-regulated the confocal imaging of T24 cell analysis. (A) confocal imaging of T24 cells treated with miRNA-21i, (B) confocal imaging of T24 cells untreatment, (C) confocal imaging of T24 cells treated with miRNA-21 mimics, Scale bar = 20 μm.

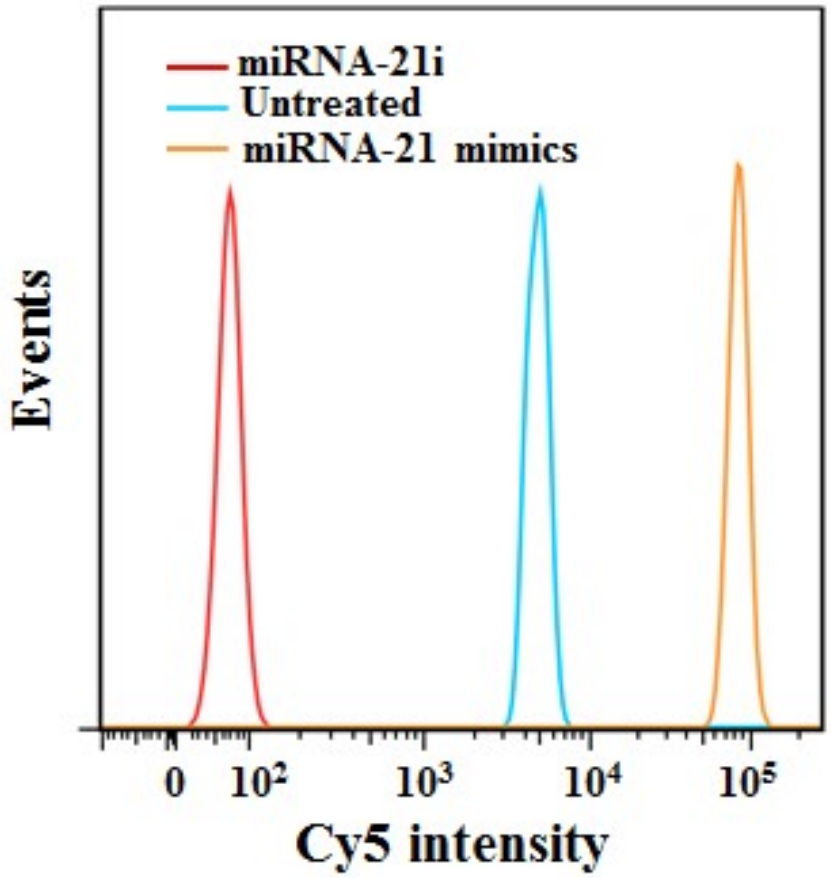

Fig. S18 miRNA-21 in T24 cells treated with miRNA-21i and miRNA-21 mimics was analyzed by flow cytometry.

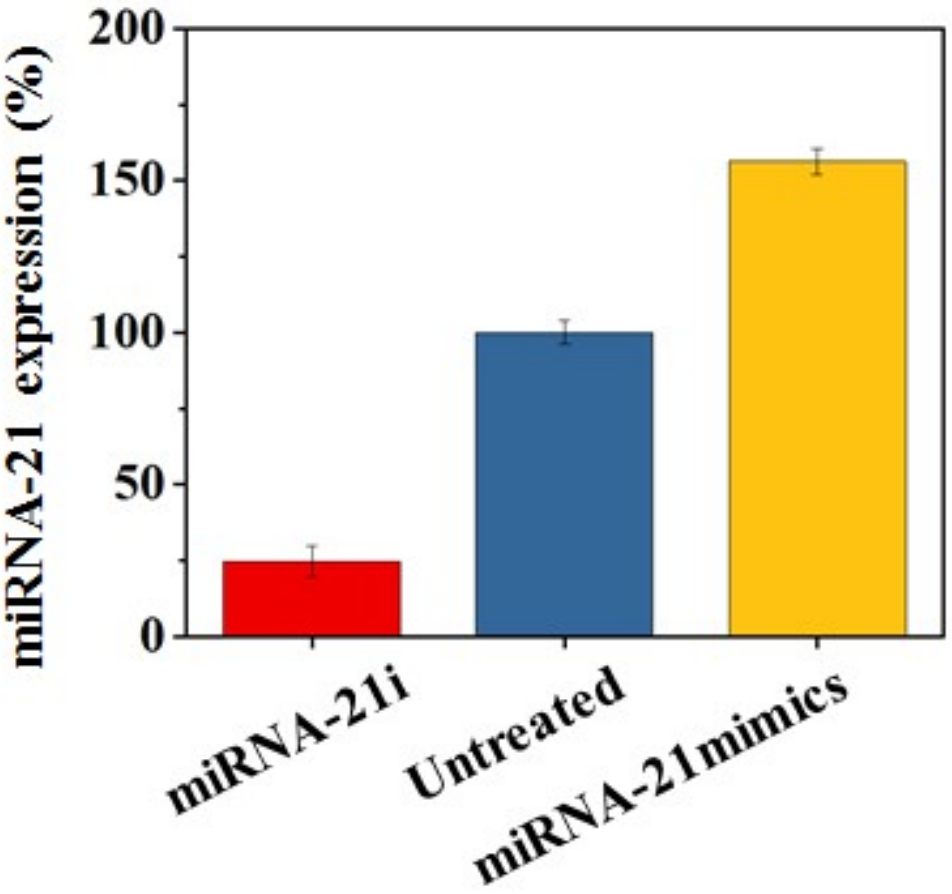

Fig. S19 Quantification of intracellular miRNA 21 expression by qRT-PCR for T24 cells with different treatment. All samples contained 5 mmol L^{-1} Mn^{2+}. Error bars were derived from N=5 experiments.

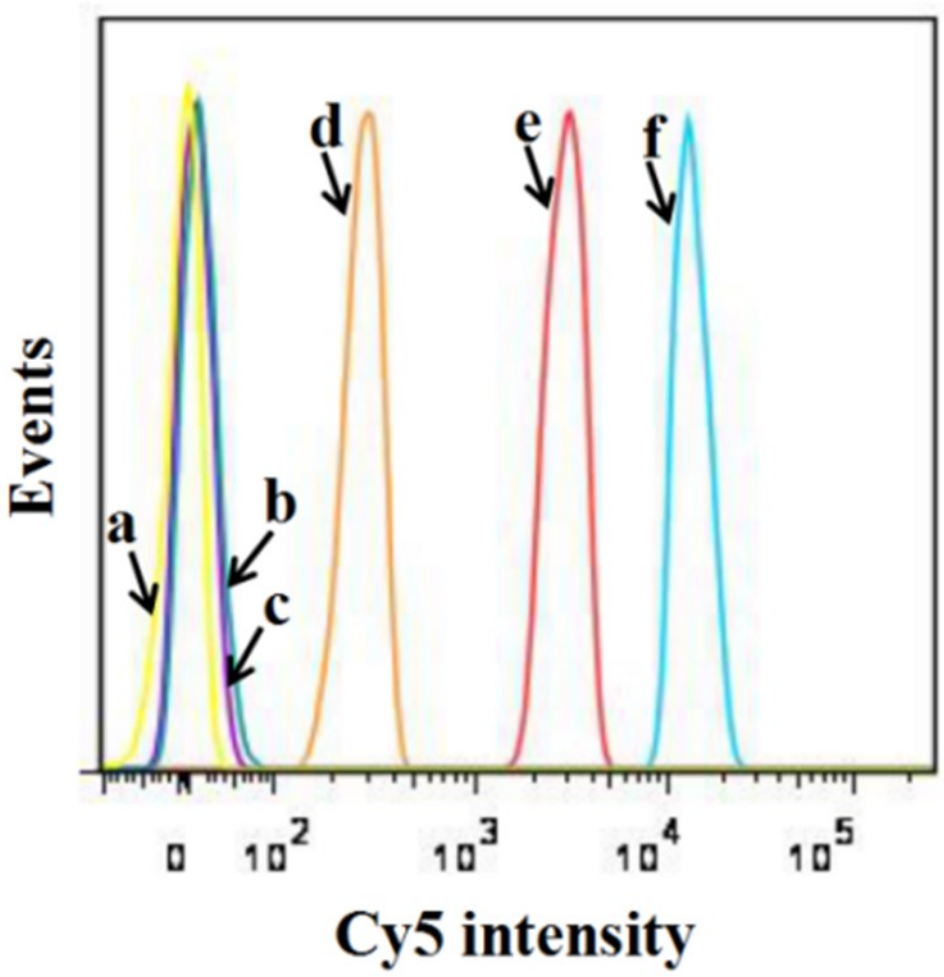

Fig. S20 Flow cytometry analysis of miRNA-21 in T24 tumor cells and HCV-29 normal cells with different sensing systems: (a) MnOx-CHA nanoprobe + HCV-29 cell; (b) MnOx-CHA-HCR nanoprobe + HCV-29 fine cell; (c) MnOx-CHA-HCR-DNAzyme nanoprobe + HCV-29 cell; (d) MnOx-CHA nanoprobe + T24 cell; (e) MnOx-CHA-HCR nanoprobe + T24 cell. (f) MnOx-CHA-HCR-DNAzyme nanoprobe + T24 cells.

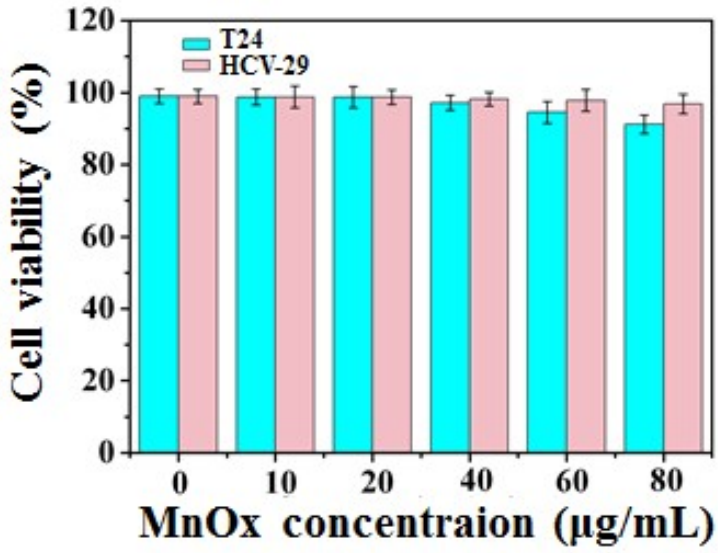

Fig. S21 Toxicity of different concentrations of MnOx nanoparticles to T24 tumor cells and HCV-29 normal cells (incubation time is 24 h). Error bars were derived from N=5 experiments.

Table S2. Comparison of the analytical performance for miRNA obtained by using this biosensor and previously reported miRNA sensing system based on different nanomaterials and different amplification strategies

Materials used	Amplification technique	Linear range	Detection limit	Reference
Cytomembrane	CHA+DNAzyme	5 pM-1 nM	1 pM	[2]
ZnO@PDA NPs	HCR+DNAzyme	0.1 fM-100 nM	0.1 fM	[3]
Cytomembrane	CHA+HCR+DNAzyme	10 pM-50 nM	5 pM	[4]
MnO_2 nanosponge	HCR+DNAzyme	10 pM-30 nM	3 pM	[5]
MnOx nanoparticle	CHA+HCR+DNAzyme	20 aM-5 pM	13 aM	This work